Volume 1 | Number 1 | Jan 2013 | Pages 1–100

Journal of
Materials Chemistry B

Materials for biology and medicine
www.rsc.org/materialsB

ROYAL SOCIETY
OF CHEMISTRY

ROYAL SOCIETY
OF CHEMISTRY

www.rsc.org/materialsB

Journal of Materials Chemistry B

ARTICLE

Hyaluronan Derivatives Bearing Variable Densities of Ferulic Acid Residues

A. Cappelli,[*,a] G. Grisci,[a] M. Paolino,[a] G. Giuliani,[a] A. Donati,[a] R. Mendichi,[b] R. Artusi,[c] M. Demiranda,[c] A. Zanardi,[c] G. Giorgi,[a] and S. Vomero.[a]

A synthetic procedure has been developed to conjugate ferulic acid (**FA**) to an important natural polysaccharide derivative such as hyaluronic acid (**HA**). The activation of **FA** with 1,1'-carbonyldiimidazole (CDI) has been investigated. Two reactive intermediates, namely monoimidazolide **2** [i. e. (*E*)-3-(4-hydroxy-3-methoxyphenyl)-1-(1*H*-imidazol-1-yl)prop-2-en-1-one] and bisimidazolide **3** [i. e. (*E*)-4-(3-(1*H*-imidazol-1-yl)-3-oxoprop-1-enyl)-2-methoxyphenyl 1*H*-imidazole-1-carboxylate] were characterized from the point of view of their structure and reactivity. The ready isolation of bisimidazolide **3** and its reactivity support its potential usefulness in the feruloylation of molecular or macromolecular materials bearing hydroxyl moieties. Bisimidazolide derivative **3** has been found to be an effective reagent in the feruloylation of **HA** to give **HAFA** graft copolymers showing different grafting degrees (GD), which could be modulated by varying the reaction conditions. A series of **HAFA** derivatives showing different GD values has been prepared and submitted to an extensive macromolecular and rheological characterization in order to ascertain that the grafting of **HA** with **FA** does not degrade the polysaccharide backbone and to evaluate the role of GD in affecting solubility and rheological properties. The results suggested that relatively low GD values were sufficient to confer physical cross-linking capabilities resulting in the features of strong gel of **HAFA** dispersions.

Introduction

Hyaluronic acid (**HA**, also called hyaluronan or hyaluronate) is a glycosaminoglycan performing several functions in human body, from the water regulation in tissues to the cellular proliferation, adhesion, differentiation, and migration. **HA** is one of the main components of the extracellular matrix and, because of its peculiar physicochemical features such as hydrophilicity and stiffness, plays a key role in the organization of cartilage proteoglycans into aggregates, providing a viscoelastic medium in the vitreous humor of the eye and synovial fluid. Moreover, the interaction of **HA** with other components of the extracellular matrix is of fundamental importance in giving the necessary compactness to derma.[1-4]

HA is synthesized by integral membrane proteins called hyaluronan synthases by repeated addition of glucuronic acid (GlcA) and N-acetylglucosamine (GlcNAc) and undergoes to a rapid turnover because enzymes called hyaluronidases actively operate its enzymatic degradation. Interestingly, the structure manipulation of the repeating unit has been reported to affect hyaluronidase activity, so that the chemical modification (e. g. crosslinking) of the biopolymer represents an interesting strategy for the modulation of in vivo stability.[5]

Ferulic acid (**FA**, 4-hydroxy-3-methoxycinnamic acid, **1**) is a hydroxycinnamic acid derivative that is naturally abundant in cell wall of several plants (i. e. in the seeds of coffee, apple, peanut, and orange, as well as in both seeds and cell walls of rice, wheat, oats, and pineapple).[6] **FA** residues are inserted in the cell wall polysaccharides through ester linkages involving its carboxylic group and the primary alcohol group of arabinose side chains of arabinoxylans playing the important role of cross-linking polysaccharides and proteins during lignin cell wall synthesis.[6-9] In particular, feruloylation is an esterification reaction mediated by specific enzymes showing an high degree of structural specificity. Furthermore, **FA** residues have been proposed to undergo peroxidase-mediated oxidative coupling (or dimerization and photoisomerism by UV light) to form a large variety of dehydrodiferulate dimers capable of bridging different polysaccharide chains.[6-9]

FA has been described to exhibit a wide range of biological and pharmacological properties including anti-inflammatory, anti-diabetic, anti-carcinogenic, anti-bacterial, anti-aging, and neuroprotective activities.[6] It is used in traditional Chinese medicine in the prevention of thrombosis and in the treatment of cardiovascular diseases. Owing to the presence of a phenol moiety linked to the conjugated side chain, **FA** is able to form resonance-stabilized phenoxy radical species, which accounts

for the potent antioxidant activity. Indeed, **FA** protects membranes from lipid peroxidation and is capable of neutralizing (scavenging) a broad range of radical species. Topical administration of **FA** was shown to inhibit UVB-induced erythema suggesting photo-protective features.[10] Finally, **FA** shows a strong absorption in the UV spectrum (maximum at 307 nm)[11] that can result into sunscreen features. The work described in the present paper is finalized to the development of a synthetic procedure for the chemical modification of **HA** with **FA** in order to obtain new advanced materials (i. e. **HAFA** graft copolymers) combining the outstanding properties of the two natural compounds. For instance, **HAFA** derivatives have demonstrated interesting wound healing properties both in vitro and in vivo preclinical models.

Experimental Section

Materials and methods

Hyaluronan starting materials were purchased from Shandong Freda Biopharm Co., Ltd, Biophil Italia SpA and used without further purifications. Melting points were determined in open capillaries and are uncorrected. Merck silica gel 60 (230-400 mesh) was used for column chromatography. Merck TLC plates, silica gel 60 F_{254} were used for TLC. NMR spectra were recorded in the indicated solvents with TMS as internal standard: the values of the chemical shifts are expressed in ppm and the coupling constants (J) in Hz.

(*E*)-3-(4-Hydroxy-3-methoxyphenyl)-1-(1*H*-imidazol-1-yl)prop-2-en-1-one (2).

To a solution of ferulic acid **1** (Sigma Aldrich, 0.39 g, 2.0 mmol) in dry THF (8.0 mL), 1,1'-carbonyldiimidazole (CDI, 0.32 g, 2.0 mmol) was added. The reaction mixture was heated under reflux for 3.5 h and then concentrated under reduced pressure (or used in the synthesis of **HAFA** derivatives without any isolation or purification). Purification of the residue by flash chromatography with dichloromethane-ethyl acetate (1:2) as the eluent gave compound **2** as a pale yellow oil, which crystallized spontaneously to form a whitish yellow solid (0.18 g, yield 37%). An analytical sample was obtained by recrystallization from chloroform by slow evaporation (mp 209 °C dec). ^{1}H-NMR (400 MHz, $CDCl_3$): 3.98 (s, 3H), 6.22 (br s, 1H), 6.88 (d, $J = 15.3$, 1H), 6.98 (d, $J = 8.3$, 1H), 7.10 (d, $J = 1.4$, 1H), 7.15 (s, 1H), 7.23 (dd, $J = 1.6, 8.3$, 1H), 7.62 (s, 1H), 8.00 (d, $J = 15.3$, 1H), 8.30 (s, 1H). ^{1}H-NMR (400 MHz, DMSO-d_6): 3.86 (s, 3H), 6.85 (d, $J = 8.2$, 1H), 7.12 (s, 1H), 7.34 (dd, $J = 1.2$, 8.2, 1H), 7.43 (d, $J = 15.5$, 1H), 7.54 (s, 1H), 7.91 (m, 2H), 8.72 (s, 1H). ^{13}C-NMR (100 MHz, $CDCl_3$): 56.1, 110.4, 111.8, 115.2, 116.4, 124.1, 126.2, 131.0, 136.2, 147.1, 149.6, 150.2, 162.0. 13C-NMR (150 MHz, DMSO-d_6): 55.9 112.1, 115.6, 116.7, 124.9, 125.5, 130.4, 137.2, 148.0, 149.5, 150.6, 162.2. MS(ESI, negative ions): m/z 243 (M-H^{+}).

(*E*)-4-(3-(1*H*-Imidazol-1-yl)-3-oxoprop-1-enyl)-2-methoxyphenyl 1*H*-imidazole-1-carboxylate (3).

To a solution of ferulic acid **1** (8.0 g, 41 mmol) in dry THF (50 mL),

1,1'-carbonyldiimidazole (CDI, 13.4 g, 82.6 mmol) was added. The reaction mixture was heated under reflux for 3.5 h and then cooled to room temperature. The white precipitate was collected by filtration, washed in sequence with dry THF and ether, and dried under reduced pressure to obtain compound **3** as a yellowish white solid (10 g, yield 72%, mp 180-182 °C). ^{1}H-NMR (400 MHz, $CDCl_3$): 3.91 (s, 3H), 7.03 (d, $J = 15.4$, 1H), 7.15 (m, 2H), 7.23 (s, 1H), 7.30 (m, 2H), 7.55 (s, 1H), 7.61 (s, 1H), 8.02 (d, $J = 15.4$, 1H), 8.28 (s, 1H), 8.30 (s, 1H). ^{1}H-NMR (400 MHz, DMSO-d_6): 3.91 (s, 3H), 7.15 (s, 1H), 7.18 (s, 1H), 7.53 (d, $J = 8.3$, 1H), 7.62 (d, $J = 8.3$, 1H), 7.69 (d, $J = 15.5$, 1H), 7.80 (m, 2H), 7.93 (s, 1H), 8.02 (d, $J = 15.4$, 1H), 8.48 (s, 1H), 8.76 (s, 1H). ^{13}C-NMR (100 MHz, $CDCl_3$): 56.2, 112.5, 116.0, 116.4, 117.6, 121.6, 123.2, 131.2, 131.4, 133.7, 136.3, 137.6, 141.0, 146.3, 148.5, 151.5, 161.5. ^{13}C-NMR (150 MHz, DMSO-d_6): 56.4, 113.2, 116.8, 117.2, 118.0, 122.6, 123.2, 130.7, 130.9, 134.0, 137.4, 137.9, 140.3, 146.3, 147.5, 151.0, 161.9. HRMS (ESI) calculated for $[C_{17}H_{14}N_4O_4 + H^+]$ requires 339.1088, found 339.1082.

Reaction of 3 with benzyl alcohol - Method A.

To mixture of **3** (0.10 g, 0.296 mmol) in dry THF (10 mL), benzyl alcohol (0.124 mL, 1.2 mmol) and triethylamine (TEA, 0.17 mL, 1.22 mmol) were added. The reaction mixture was stirred at room temperature under argon atmosphere for 5 days and then concentrated under reduced pressure. The resulting residue was purified by flash chromatography with dichloromethane-ethyl acetate (2:1) as the eluent to give benzyl 1-imidazolecarboxylate (**4**) as a colorless oil (0.031 g, yield 52%). The spectroscopic (^{1}H and ^{13}C NMR spectra) features of this compound were in agreement with those described in the literature.[12,13] The same flash chromatography purification of the reaction mixture with dichloromethane-ethyl acetate (1:2) as the eluent afforded compound **2** as a pale yellow oil, which crystallized spontaneously to form a whitish yellow solid (0.027 g, yield 37%).

Reaction of 3 with benzyl alcohol - Method B.

To mixture of **3** (0.10 g, 0.296 mmol) in dry THF (10 mL), benzyl alcohol (0.124 mL, 1.2 mmol) and 1,8-diazabicyclo[5.4.0]undec-7-ene (DBU, 0.18 mL, 1.2 mmol) were added. The reaction mixture was refluxed under argon atmosphere for 3 h and then concentrated under reduced pressure. The resulting residue was partitioned between chloroform and water and the organic layer was washed with water, dried over sodium sulfate and concentrated under reduced pressure. Purification of the final residue by flash chromatography with dichloromethane as the eluent gave benzyl 3-(4-hydroxy-3-methoxyphenyl)-2-propenoate (**5**)[14] as a colorless oil (0.037 g, yield 43%). ^{1}H-NMR (400 MHz, $CDCl_3$): 3.90 (s, 3H), 5.24 (s, 2H), 5.92 (br s, 1H), 6.33 (d, $J = 15.9$, 1H), 6.89 (d, $J = 8.2$, 1H), 7.02 (d, $J = 1.5$, 1H), 7.07 (dd, $J = 1.5, 8.2$, 1H), 7.39 (m, 5H), 7.65 (d, $J = 15.9$, 1H). ^{13}C-NMR (100 MHz, $CDCl_3$): 55.9, 66.3, 109.4, 114.8, 115.2, 123.2, 127.0, 128.3, 128.6, 136.2, 145.3, 146.8, 148.1, 167.1. MS(ESI): m/z 307 (M+Na^{+}).

General procedure for the synthesis of HAFA derivatives. A mixture of **HA** sodium salt in formamide (20 mL/1 g **HA**) was heated at about 58-60 °C until the complete dissolution and cooled to room temperature. To the resulting viscous solution, TEA (1 equivalent) and the appropriate amount of the suitable activated derivative of **FA** were added in sequence. In particular, compound **2** was used as activation reaction mixture without any isolation or purification (Table 1), whereas compound **3** was added as a finely powdered solid (entry 1 of Table 2) or as a dispersion in formamide (entries 2-9 of Table 2). The reaction mixture was stirred overnight at room temperature and then diluted with a 5% w/v NaCl solution (5 mL/1 g **HA**). The resulting mixture was stirred at room temperature for 10-15 min and MeOH was added to decrease mixture viscosity when necessary. Finally, the polymer was obtained by treatment of the mixture with acetone and purified by washing with MeOH for three times. The final solid was dried under reduced pressure to afford the expected **HAFA** derivative.

X-ray crystallography. A single crystal of **2** was submitted to X-ray data collection by using a four-circle diffractometer at 293K, equipped with a graphite monochromated Mo-Kα radiation (λ = 0.71069 Å). The structure was solved by direct methods implemented in the SHELXS-97 program.[15] Data refinement was carried out by full-matrix anisotropic least-squares on F^2 for all reflections for non-H atoms by means of the SHELXL-97 program.[16]

Crystallographic data (excluding structure factors) for the structure in this paper have been deposited with the Cambridge Crystallographic Data Centre as supplementary publication no. CCDC 950542. Copies of the data can be obtained, free of charge, on application to CCDC, 12 Union Road, Cambridge CB2 1EZ, UK; (fax: + 44 (0) 1223 336 033; or e-mail: deposit@ccdc.cam.ac.uk).

Mass Spectrometry. Electrospray measurements have been carried out on a LCQ-DECA ion trap (ThermoFinnigan, Bremen, D) and on a LTQ Orbitrap XP instrument (ThermoFinnigan, Bremen, D). Operating conditions for the ESI source were as follows: spray voltage +/- 4.5 kV; capillary temperature 200°C; sheath gas (nitrogen) flow rate, ca. 0.75 L/min.

MS^n product ion experiments have been carried out inside the ion trap by isolating the precursor ion and then by applying a supplementary potential for collision induced dissociations; collision gas: He; collision energy: 20-40% arbitrary units. The mass window was 1 or 2 u. The Orbitrap analyzer was operating in the resolution range 30,000-100,000 FWHM and calibrated using the manufacturer's calibration mixture obtaining mass accuracies < 2 ppm. 30-50 Scans were recorded and averaged for accurate mass measurements.

Methanolic solutions of the different compounds (ca. 1×10^{-4} M) have been introduced via direct infusion at a flow rate of 5 μL/min.

Chromatographic system. The characterization of the molecular weight distribution (MWD) of two native **HA** samples and six **HAFA** derivatives was performed by a multi-angle laser light scattering (MALS) absolute detector on-line to a size exclusion chromatographic system (SEC). The MWD was obtained by a modular multi-detector SEC system. The SEC system consisted of an Alliance 2695 separation module equipped with two on-line detectors: a MALS Dawn DSP-F photometer and a 2414 differential refractometer (DRI) used as concentration detector. The setup of this multi-detector SEC system was serial in the following order: Alliance-MALS-DRI. In a multi-detector SEC system the different on-line detectors have an intrinsic temporal delay because they are located in different positions of the fluidic path. Consequently an alignment of the different signals is needed. The experimental methodology for a reliable use of the SEC-MALS system has been described in detail in the literature.[17-21]

The SEC-MALS experimental conditions were the following: 3 TSKgel PW (G6000-G5000-G4000) from Tosoh Bioscience as column set; 80% 0.20M NaCl + 20% dimethylsulfoxide (DMSO) as mobile phase; 0.8 mL/min of flow rate; 150 μL of injection volume; ca. 1 mg/mL of sample concentration.

The MALS detector uses a vertically polarized He-Ne laser, λ = 632.8 nm, and simultaneously measures the intensity of the scattered light at 18 fixed angular locations ranging in mixed solvent from 12.4° to 155.4°. It is well known that an on-line MALS detector coupled to a concentration detector allows to obtain the true molecular weight M and the size, i. e. the root mean square radius $<s^2>^{1/2}$ in short to hereafter denoted as radius of gyration Rg, of each fraction of the eluting polymer. The MALS calibration constant was calculated using Toluene as standard assuming a Rayleigh Factor $R(\theta)=1.406 \cdot 10^{-5}$ cm^{-1}. The normalization of the photodiodes was performed by measuring the scattering intensity in the mobile phase of a bovine serum albumin (BSA: M = 66.4 kg/mol, Rg = 2.9 nm) globular protein assumed to act as an isotropic scatterer. The MALS photometer has been described in detail in the literature.[19,20]

The specific refractive index increment, dn/dc, with respect to the mobile phase was measured by a Chromatix KMX-16 differential refractometer. The dn/dc value in 0.20 M NaCl+DMSO (80:20) solvent at 35 °C of temperature was: 0.115 mL/g for native **HA**; 0.110 mL/g for **HAFA** derivatives.

Rotational Rheometer. The rheological properties in oscillation mode (frequency sweep) were measured by means of an AR 2000 rotational rheometer from TA Instrument using a cone/plate geometry. The rheological properties were measured on concentrated solution/dispersion of native HA or HAFA derivative samples. The sample temperature was maintained at 20 °C by a Peltier Plate. The rheological experimental conditions were the following: i) rotor: cone/plate, stainless steel material, 4 cm diameter, 1° angle; ii) temperature 20 °C; iii) method: frequency (ω) sweep from 0.01 rad/s to 620.3 rad/s; iv) sample concentration 2%.

Results and Discussion

This journal is © The Royal Society of Chemistry 2012

J. Mater. Chem. B, XXXX, **XX**, X-X | **3**

Synthesis and characterization of activated derivatives of FA. The reaction of **FA** (**1**) with one equivalent of 1,1'-carbonyldiimidazole (CDI) in refluxing dry THF led to the formation of the corresponding *N*-acylimidazole **2** (Scheme 1), which was characterized by NMR spectroscopy, mass spectrometry (MS), and by crystallography (see below). However, purification of this important intermediate required the application of chromatographic techniques (i. e. flash chromatography) and the yields were found to be relatively low.

On the other hand, when two equivalents of CDI were employed, we observed the formation of a conspicuous amount of a yellowish-white precipitate, which was easily collected by filtration, washed with dry THF and diethyl ether, dried under reduced pressure, and stored into a tightly closed vial.
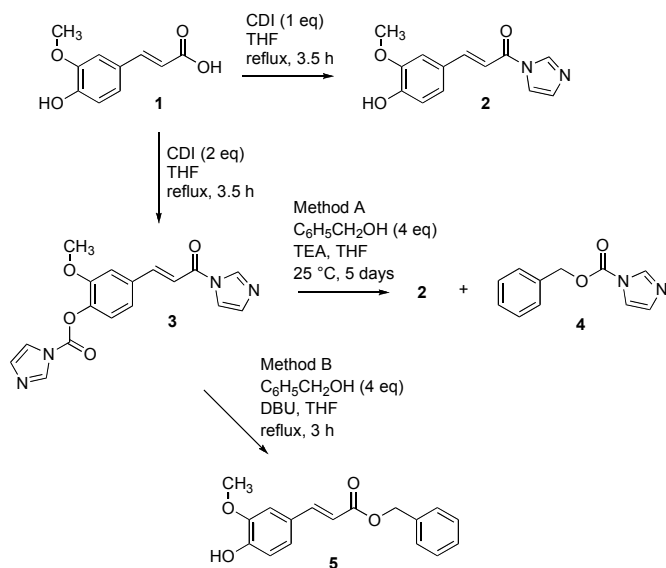

Scheme 1. Activation of **FA** and reactivity of compound **3**.

The solid was characterized by both NMR spectroscopy (^{1}H, ^{13}C, COSY, NOESY, HSQC, and HMBC experiments) and MS. Accurate mass measurements suggested the formula $C_{17}H_{14}N_4O_4$ that was also supported by NMR experiments. The results were easily explained in terms of capability of the phenol group of **2** to react with the second equivalent of CDI to give 1-imidazolecarboxylate **3**. The easy isolation of **3** as a solid from the reaction mixture led us to consider this compound a promising intermediate for the insertion of ferulic acid residues in different molecular or macromolecular materials. The reaction of **3** with low-molecular weight alcohols such as benzyl alcohol revealed the higher reactivity of the activated carbamate moiety with respect to the *N*-acryloylimidazole one. In fact, the reaction of **3** with benzyl alcohol in THF in the presence of triethylamine (TEA) at room temperature (Method A) gave a mixture of **2** and benzyl 1-imidazolecarboxylate (**4**).[12,13] In other words, benzyl alcohol behaved as a scavenger in restoring the phenol hydroxyl moiety. The same reaction with 1,8-diazabicyclo[5.4.0]undec-7-ene (DBU, in place of TEA) in refluxing THF (Method B) afforded benzyl ester **5**[14] supporting the potential usefulness of **3** for introducing ferulic acid residues in molecular or macromolecular materials bearing hydroxyl moieties.

The crystal structure of **2** (Figure 1) confirmed the trans configuration of the double bond. Bond lengths and bond angles were found to be normal.

As an example, the bond distances C(6)-N(1) and C(6)-C(7) were 1.421(4) and 1.460(4) Å, respectively. The 2-methoxy-4-vinylphenol moiety was planar but the imidazole ring was out of the plane. The dihedral angle between the least squared planes defined by the phenyl and the imidazole was 23.2(2)°. The crystal structure consisted of chains of molecules linked by hydrogen bonding interactions O(3)-H(x,y,z)···N(3) (3/2+x,1/2-y,1/2+z) with the H···N distance equal to 2.678(4) Å. Unusual hydrogen bond interactions C(5)-H(5)···O(1) (1/2-x,1/2+y,1/2-z) linked the chains together with the H···O distance equal to 2.875(4) Å.
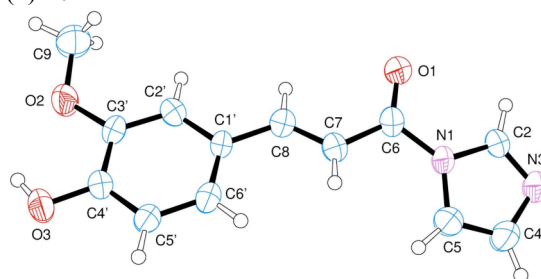
Figure 1. X-ray crystal structure of **2**. Ellipsoids enclose 50% probability.

Mass spectrometry was used to evaluate the reactivity of protonated **2** and **3** in the gas phase. Owing to electrospray in positive mode, only the protonated molecules of **2** and **3** were observed. Low-energy collision-induced dissociation MS^n experiments, carried out inside an ion trap, were used for elucidating the reactivity of different ionic species (Figure 2).
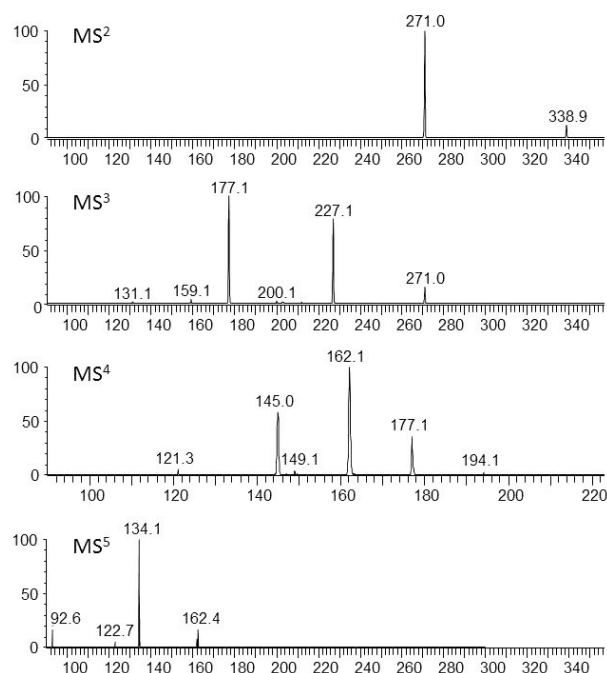
Figure 2. Low-energy collision-induced dissociation MS^n spectra obtained by selecting different precursor ions produced by **3**.

The MS^2 spectrum, obtained by selecting $[3+H]^+$ (*m/z* 339) as precursor ions, showed product ions at *m/z* 271 attributable

to elimination of imidazole. This behavior was identical of that shown by $[2+H]^+$ in which only an imidazole residue is present. In the case of **3**, it was of interest to determine which of the two imidazolyl moieties was involved in this fragmentation. The MS^3 spectrum, obtained by selecting the species at m/z 271 as precursor ions, showed the most abundant product ions at m/z 227 and 177, due to elimination of 44 and 94 u, respectively. The former are due to loss of CO_2, thus evidencing that the imidazole bound to the carboxyl group is the first to be eliminated by $[3+H]^+$.

Ions at m/z 177 are due to the elimination of an imidazolecarbaldehyde molecule. These latter can further decompose (MS^4) through an unusual loss of a methyl radical from an even-electron species, or losing methanol, yielding the ionic species at m/z 162 and 145, respectively. The radical cations at m/z 162 can further decompose (MS^5) by elimination of 28 u yielding ions at m/z 134.

Reaction of FA activated derivatives 2 and 3 with HA

In the development of an easily scalable, industrially-viable functionalization procedure, commercially available sodium hyaluronate was dissolved into formamide at 58-60 °C, and the resulting viscous solution was cooled to room temperature and treated in sequence with triethylamine (TEA) and the reaction mixture containing activated **FA** derivative **2**.
The stoichiometric ratio between **2** and **HA** (**2/HA** ratio) was varied from 1:1 to 1:4 (i. e. 100, 50, and 25%, see Table 1) in order to obtain graft copolymers showing a different grafting degree (GD). Moreover, different amounts of the starting materials were used in the aim of evaluating the productive conversion of the 1-acylimidazole derivative **2** into ferulate. The data shown in Table 1 suggest that GD was substantially regulated by **2/HA** stoichiometric ratio, which affected also the productive conversion of the 1-acylimidazole derivative **2** into ferulate. In fact, low **2/HA** ratios (i. e. 25%) produced low GD (i. e. 7%) and relatively high conversion values (i. e. 28%), whereas high **2/HA** ratios (i. e. 100%) led to higher GD (i. e. 15%) and lower conversion values (i. e. 15%). However, when **HAFA** samples thus obtained were submitted to hydrolytic conditions, the presence of impurity traces was observed in the ^{1}H NMR spectra. This result was related to the use of crude **2**

(as reaction mixture, without any purification) in the grafting reaction.
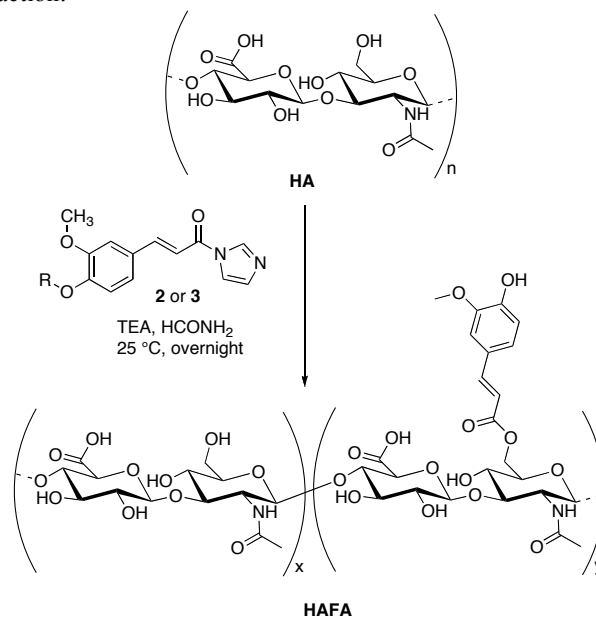
Scheme 2. Esterification of **HA** into **HAFA** derivatives.

The easy isolation of **3** in its pure form and the reactivity shown above led to evaluate the use of this compound in **HA** grafting reaction. Thus, the viscous solution of sodium hyaluronate in formamide was treated in sequence with TEA and activated **FA** derivative **3**. Owing to the limited solubility shown by **3** in formamide, the reactant was added to the reaction mixture as a finely powdered solid or as a dispersion in formamide. The stoichiometric ratio between **3** and **HA** (**3/HA** ratio) was varied from 75 to 10% (see Table 2) with a number of five replicates (with different **HA** amounts) in **3/HA** ratio of 20% in the aim of optimizing the conditions to obtain a desired grafting degree (GD) and to maximize the productive conversion of **3** into ferulate.

Table 1. Reaction parameters in the functionalization of **HA** polymer to **HAFA** graft copolymers with *N*-acylimidazole **2**.

entry	graft copolymer	HA[a] (g)	HA (mmol)	2/HA ratio (%)	grafting degree[b] (%)	convers.[c] (%)
1	**HAFA**-01	3.0	7.5	100	15	15
2	**HAFA**-02	3.0	7.5	50	11	22
3	**HAFA**-03	3.0	7.5	25	7	28
4	**HAFA**-04	10	25	50	12	24

[a] All **HAFA** graft copolymers were obtained by using **HA**-02 as the starting material. [b] A rough estimate of the grafting degree was made by ^{1}H-NMR spectroscopy after hydrolysis with NaOD in D_2O as described below in the main text. [c] The conversion into ferulate was calculated from the substitution degree and stoichiometric ratio **2/HA**.

This journal is © The Royal Society of Chemistry 2012

J. Mater. Chem. B, XXXX, **XX**, X-X | **5**

Table 2. Reaction parameters in the functionalization of **HA** polymer to **HAFA** graft copolymers with activated **FA** derivative **3**.

entry	graft copolymer	HA[a] (g)	HA (mmol)	3/HA ratio (%)	grafting degree[b] (%)	convers.[c] (%)
1	**HAFA**-07	3.0	7.5	75	17	23
2	**HAFA**-08	10	25	60	15	25
3	**HAFA**-09	1.6	4.0	40	12	30
5	**HAFA**-10	3.0	7.5	20	8	40
4	**HAFA**-14	9.0	22.4	20	8	40
6	**HAFA**-11	10	25	20	8	40
7	**HAFA**-15	10	25	20	5	25
8	**HAFA**-12	15	37.4	20	4	20
9	**HAFA**-13	30	75	10	3	30

[a] All **HAFA** graft copolymers were obtained by using **HA**-01 polymer except the **HAFA**-15 derivative, obtained by using **HA**-02 polymer. [b] A rough estimate of the grafting degree was made by ^{1}H-NMR spectroscopy after hydrolysis with NaOD in D_2O as described below in the main text. [c] The conversion into ferulate was calculated from the substitution degree and stoichiometric ratio **3**/**HA**.

The comparative analysis of the data reported in Tables 1 and 2 suggested that the use of **3** produced GD values higher than those obtained with **2**. Moreover, as observed in **HA** grafting with **2**, the **3**/**HA** stoichiometric ratio affected both GD and the productive conversion of **3** into ferulate in such a way that high **3**/**HA** ratios (i. e. 75%) led to high GD (i. e. 17%) and to relatively low conversion values (i. e. 23%), while gradual decreases in GD values and increases in the productive conversion were observed with the decrease of **3**/**HA** ratios. The data obtained with the five replicates with **3**/**HA** ratio of 20% appeared to suggest that the scalability of the process was not optimized. Owing to the relatively low solubility of **3** in formamide, the heterogeneity of the reaction mixture requires additional work to be performed in order to optimize further the conversion of the imidazolide into ferulate.

Structure of HAFA derivatives

The structure of **HAFA** derivatives was characterized by ^{1}H NMR spectroscopy using D_2O as the solvent. The NMR analysis of all the graft copolymers mentioned in the present paper confirmed the successful coupling between **HA** and **FA** in our reaction conditions. In fact, beside the distinctive profile of **HA** in the up-field region, signals attributable to the **FA** residues were well manifest in the down-field region of the recorded spectra. Moreover, the addition of free **FA** to **HAFA**-14 dispersion in D_2O (Figure 3) showed that the signals of free **FA** displayed chemical shift values different from those of **FA** bound to the polysaccharide. The highest difference involved the signals attributed to the *trans*-double bond protons (in particular to H in position beta of the acryloyl moiety) in agreement with the assumption that the ferulate residues are linked through ester bonds to HA.

Determination of HAFA grafting degree by ^{1}H NMR spectroscopy

In order to estimate GD of **HAFA** derivatives, the hydrolysis of their ester linkages with **FA** moieties were performed in D_2O by using NaOD and it was followed by ^{1}H NMR spectroscopy. Thus, **HAFA** samples (ca. 6 mg) were swollen in D_2O (ca. 0.7 mL) and a drop of a 40% NaOD in D_2O was added (Figure 4). ^{1}H NMR spectra of the dispersions were recorded at regular time intervals until the end of the hydrolysis. The down-field signals attributed to ferulate were integrated and the integral values were compared with that of the methyl group of *N*-acetyl residue of **HA**. During the performing of this experiment we observed that the addition of 40% NaOD solution to the **HAFA** dispersion in water produced marked modifications in the samples. In particular, the starting colorless transparent gel sample became a viscous yellow solution immediately after the adding up of the base and the color disappeared in the following time with the completion of the hydrolysis reaction. These results were rationalized by assuming that the basic environment was capable of deprotonating the phenol hydroxyl of ferulate residues and breaking the H-bond network, which stabilizes the gel dispersion.

6 | *J. Mater. Chem. B*, XXXX, **XX**, X-X

This journal is © The Royal Society of Chemistry 2012
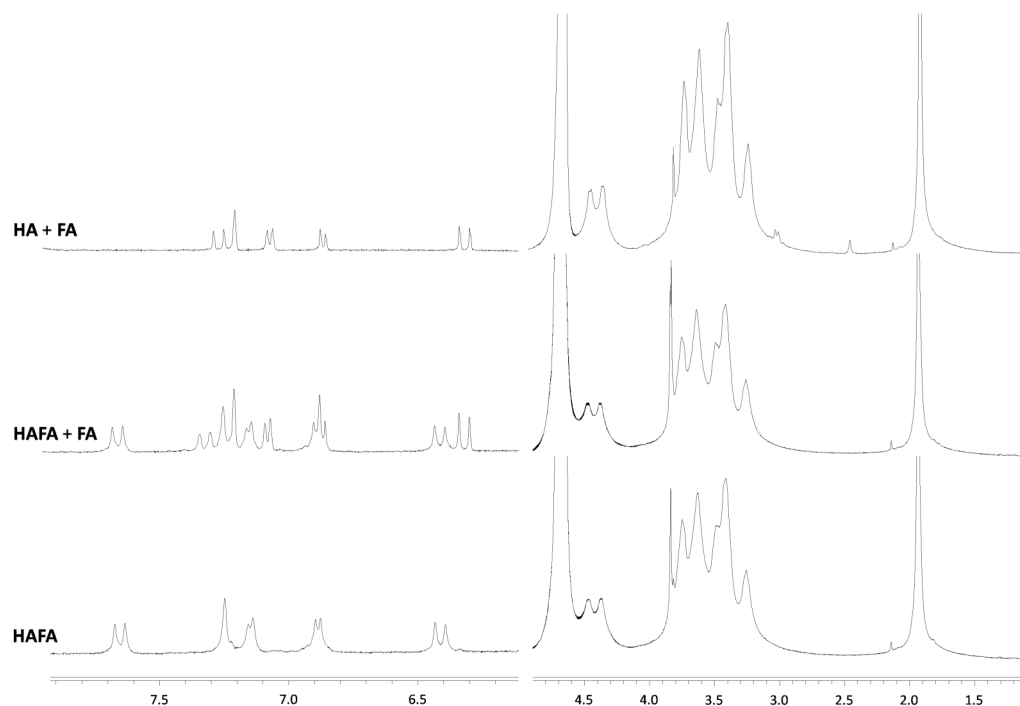
Figure 3. Comparison of ^{1}H NMR spectra obtained with **HAFA**-14 derivative (D$_2$O, 400 MHz) in the absence (bottom trace), or in the presence (middle trace) of free **FA** (added) with that obtained with a physical mixture of **HA** and **FA** (top trace). The peak intensity of the aromatic regions was magnified (x 2) for the sake of clarity.
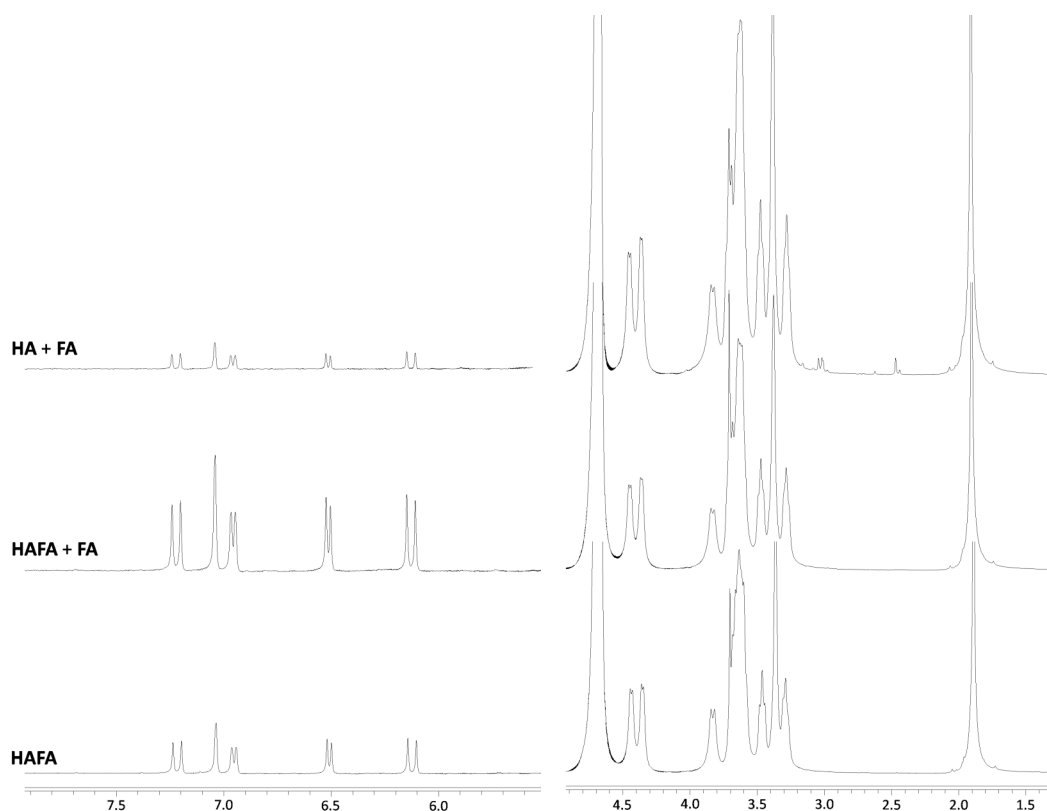
Figure 4. Effects produced by the NaOD addition on the ^{1}H NMR spectra (D$_2$O, 400 MHz) of Figure 3 samples. The dispersions of **HAFA**-14 derivative (bottom trace), **HAFA**-14 containing free **FA** (middle trace), and the physical mixture of **HA** and **FA** (top trace) were treated with a drop of a 40% NaOD in D$_2$O and ^{1}H NMR spectra were recorded at regular time intervals until the end of the hydrolysis. The peak intensity of the aromatic regions was magnified (x 2) for the sake of clarity.

This journal is © The Royal Society of Chemistry 2013

J. Mater. Chem. B, XXXX, **XX**, X-X | **7**

Macromolecular characterization of HAFA derivatives

Solubility of HAFA derivatives

Specifically for the macromolecular characterization, but also in general for the derivatives processing and the knowledge of complex solution properties, the solubility of **HAFA** graft copolymers in aqueous solvents is very important. The solubility of **HAFA** derivatives was tested in two different solvents: 1) 0.2 M NaCl (usual aqueous solvent for **HA** native biopolymers); 2) 80% 0.2 M NaCl + 20% DMSO mixed solvent (an expected better solvent for **HAFA** derivatives). The solubility data of native **HA** and **HAFA** derivatives are reported in Table 3. The solubility data were obtained by quantification of the Recovered Mass,[22] that is the mass of polymeric sample eluting from the SEC columns expressed in % with respect to the injected mass (calculated from the product of sample concentration and injection volume). The Recovered Mass is calculated from the area of the chromatogram of the differential refractometer (DRI) concentration detector after accurate calibration. In general it is well known that the Recovered Mass is lower than 100% in consequence of the presence in the sample of solvents, additives and impurity. In particular **HA** samples always contain a meaningful fraction of water (ca. 5-15%).

The two native **HA** samples were completely soluble both in 0.2M NaCl aqueous solvent and in the mixed solvent containing 20% of organic DMSO. On the contrary, **HAFA** derivatives showed very different behaviors. The solubility degree of **HAFA** derivatives is substantially related to GD value.

Specifically, **HAFA** derivatives showing the lowest GD value (*e. g.* **HAFA**-12 and **HAFA**-13: GD ≤ 4%) were completely soluble, whereas **HAFA**-15 showing a GD value around 5% was partially soluble, and those showing higher GD values (*e. g.* **HAFA**-10, **HAFA**-11, and **HAFA**-14: GD = 8%) could be considered practically insoluble. Furthermore, a little better solubility of **HAFA** derivatives was obtained by using the mixed solvent 0.20 M NaCl-DMSO (80:20), whereas a more significant increase in solubility was obseved when *N*,*N*-dimethylacetamide (DMA) was used as the co-solvent in the (50:50) ratio with 0.05M NaCl water solution (data not shown). In consideration of the hydrogen bond acceptor features, which are generally recognized to DMA, this result suggests that the feruloylation of **HA** into **HAFA** graft copolymers induced the formation of physical cross-linking based on the establishment of interchain hydrogen bonds, which are broken by the addition of substantial amounts of a strong acceptor such as DMA. In conclusion, the density of ferulate residues appears to affect significantly the intermolecular interactions of **HAFA** derivatives and their behavior in water environment.

Macromolecular and conformational characterization

The macromolecular and conformational characterization of **HAFA** derivatives as well as of the **HA** starting biopolymer were performed by means of a multi-angle laser light scattering (MALS) absolute detector on-line to a size exclusion chromatography (SEC) system. The SEC-MALS characterization was performed by using as mobile phase the mixed solvent 0.2 M NaCl-DMSO (80:20), considering the little better solubility in this solvent of the **HAFA** derivatives. Table 4 summarizes the most important SEC-MALS results obtained with native **HA** and **HAFA** samples. Specifically, Table 4 reports the molecular weight of the peak of the chromatogram (M_p), the weight-average of the molecular

weight (M_w), and the dispersity M_w/M_n where M_n denotes the numeric-average of the molecular weight.

Table 3. Solubility data of **HA** native and **HAFA** derivative samples calculated from the Recovered Mass.

polymer	grafting degree (%)	0.2M NaCl (%)	0.2M NaCl-DMSO (80:20) (%)
HA-01		88	89
HA-02		94	92
HAFA-07	17	Insoluble	Insoluble
HAFA-08	15	Insoluble	Insoluble
HAFA-09	12	Insoluble	Insoluble
HAFA-10	8	4.2	8.2
HAFA-11	8	3.0	8.9
HAFA-14	8	9.4	32
HAFA-15	5	37	68
HAFA-12	4	87	88
HAFA-13	3	81	81

Table 4. Macromolecular features of the **HAFA** derivatives compared to the starting **HA**.

polymer	grafting degree (%)	Sol. (%)	Mp (kg/mol)	Mw (kg/mol)	Mw/Mn
HA-01		89	164.2	249.8	3.2
HA-02		92	211.9	271.2	3.1
HAFA-13	3	81	181.7	299.9	2.8
HAFA-12	4	88	213.1	283.3	3.0
HAFA-15	5	68	225.4	365.1	3.9
HAFA-14	8	32	143.6	232.1	3.8
HAFA-11	8	8.9	100.2	119.2	2.4

In the analysis of macromolecular data reported in Table 4 some important concerns have to be considered. Obviously the SEC-MALS results (MWD, relative averages and dispersity) only refer to the soluble fraction of the **HAFA** derivative samples. The direct consequence of the partial solubility is that the molecular weight and dispersity of some derivatives could

This journal is © The Royal Society of Chemistry 2013

J. Mater. Chem. B, XXXX, **XX**, X-X | **8**

be underestimated. Furthermore, no information on the MWD of the completely insoluble **HAFA** derivatives could be obtained. Despite the above mentioned problems in the solubility of **HAFA**-derivatives, the macromolecular SEC-MALS results (Table 4) for native **HA** and **HAFA** derivatives convey important information. The molecular weight of the two native **HA** samples is high (M_w average ca. 260 kg/mol) and their MWD is broad (M_w/M_n ca. 3). Furthermore, their MWD were found to be substantially similar. In general, the comparison of the differential MWD of completely soluble samples (**HA**-01, **HA**-02, **HAFA**-12, and **HAFA**-13, see Table 4) clearly shows that the derivatization of **HA** does not change the molecular weight of **HA** macromolecules. In other words, the derivatization does not degrade the **HA** polysaccharide backbone. Some little differences in MWD could be explained by the partial solubility (**HAFA**-14) and by the presence in the solution of some fractions of **HAFA** macromolecules showing low physical cross-linking density (**HAFA**-15).

Table 5 reports the parameters (e. g. the average size Rg of macromolecules, the intercept K and the slope α of the conformation plot) of the experimental function Rg = f(M) generally known as conformation plot. The conformation plot, Rg = K·M$^\alpha$, is the scaling law between the size Rg and chain length (molecular weight) of macromolecules. In general the conformation plot is very important because is related with the conformation, branching, and eventual derivatization or chemical modification of the polymer.

**Table 5.** Size and conformation results of starting **HA** and of some **HAFA** derivatives.

polymer	grafting degree (%)	Sol. (%)	Mw (kg/mol)	Rg (nm)	K	α
HA-01		89.2	249.8	49.6	3.46E-02	0.58
HAFA-13	3	81.2	299.9	51.4	4.33E-02	0.56
HAFA-12	4	87.6	283.3	48.9	3.75E-02	0.57
HAFA-15	5	68.2	365.1	54.1	6.59E-02	0.52
HAFA-14	8	32.1	232.1	41.1	4.49E-02	0.55

The derivatization of **HA** with **FA** produces only little changes in the conformation of the native **HA** macromolecules. Indeed, the slope α of the conformation plot in the mixed solvent decreases a little from 0.58 to 0.55. Thus, **HAFA** macromolecules are a little more compact with respect to the native **HA** ones. Furthermore, the conformation plot confirms that in the **HAFA**-15 derivative there is a little extent of physical cross-linking (more compact conformation, slope α ca. 0.52). Obviously, the conformation plot concerns only the soluble macromolecule fractions of **HAFA** samples.

Rheological properties

Figure 5 shows the comparison of the experimental rheological curve of complex dynamic viscosity |η*| as a function of the frequency ω for two **HA** native samples and six **HAFA** derivatives. The |η*|=f(ω) rheological curves were

obtained using concentrated solution or dispersion of native **HA** and **HAFA** derivatives in the mixed solvent 0.2M NaCl-DMSO (80:20). The specimens subjected to the rheological test were substantially gels with 2% of sample concentration. Specifically, the rheological characterization allows to overcome the solubility problems of **HAFA** derivatives showing high GD values.
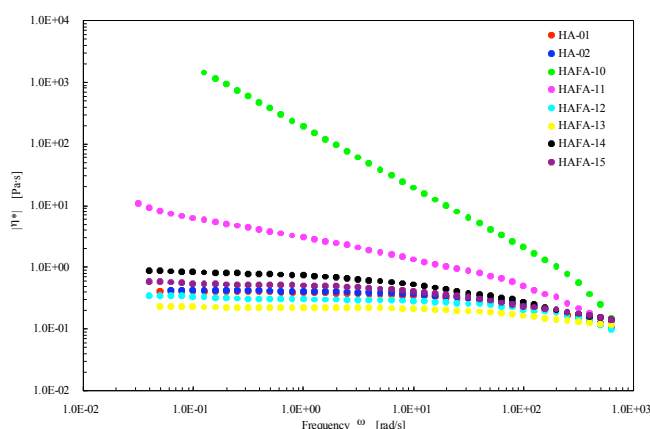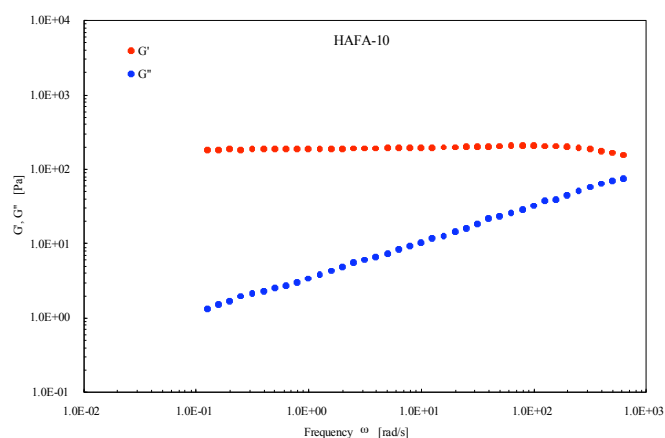

Figure 5. Complex dynamic viscosity |η*| as a function of the frequency ω of native **HA** samples and **HAFA** derivatives.

The comparison of the experimental |η*|=f(ω) rheological curve of the two native **HA** samples with six **HAFA** derivatives with different GD values (see Figure 5) shows a very different rheological behavior apparently related to GD of **HAFA** derivatives. The rheological curve of the two native **HA** samples are very similar in consequence of the quite similar MWD (see data in Table 3). The rheological curve of two **HAFA** derivatives with low GD (**HAFA**-12, GD = 4; **HAFA**-13, GD = 3) is a little shifted toward lower complex dynamic viscosity values without meaning modifications of the pseudo plastic behavior of the polymer. Evidently, in these **HAFA** derivatives showing low GD values, the grafting with **FA** residues is particularly effective in affecting their rheology. The rheological curve of **HAFA** derivatives with intermediate GD values is only shifted toward higher complex viscosity values. Evidently, when GD > 4% also a low degree of physical cross-linking is present without compromising the complete solubility of samples. Finally, when GD ≥ 8% the physical cross-linking degree increases, the complex viscosity strongly increase, and the solubility also in the mixed solvent is only partial.

Figures 6 and 7 show the comparison between the elastic or in-phase (G') moduli and the viscous or out-phase moduli (G'') for the native **HA**-02 sample and for the **HAFA**-10 derivative respectively. The native **HA**-02 sample shows a typical mechanical spectrum of a high molecular weight biopolymer with a crossover point (G'=G''). On the contrary the mechanical spectrum of the **HAFA**-10 derivative (GD = 8%) is completely different with the elastic moduli G' higher than the viscous moduli G'' for the whole range of frequency explored. This behavior is typical of a "strong" gel. This rheological result confirms the presence of physical cross-linking in **HAFA** derivatives showing GD values higher than around 8%. Therefore, the insolubility of **HAFA** derivatives showing the highest GD values (GD > 10%) can be rationalized in terms of presence of a high degree of physical cross-linking, which could be originated by the non-covalent interaction of ferulate residues building a stable H-bond network.

This journal is © The Royal Society of Chemistry 2012

J. Mater. Chem. B, XXXX, **XX**, X-X | **9**

Figure 6. Comparison between elastic (G') and viscous (G")
moduli for native **HA**-02 sample.

Figure 7. Comparison between elastic (G') and viscous (G")
moduli for **HAFA**-10 derivative.

This assumption was supported by the effects observed in
the rheological behavior when *N,N*-dimethylacetamide was
used as the co-solvent in the (50:50) ratio with 0.05M NaCl
solution. In short, DMA was capable of decreasing the apparent
cross-linking degree of **HAFA** derivatives up to the
corresponding values shown by native **HA** samples (data not
shown). Thus, in the aqueous dispersions of **HAFA** derivatives,
ferulic residues are prone to establish interchain hydrogen
bonds, which are broken by DMA.

Resistance against enzymatic degradation

The presence of microorganisms on the epidermis causes a
relevant biological activity on the skin, activity which takes the
form of various enzymatic functions, including the one carried
out by the enzyme hyaluronidase. **HA** is naturally degraded due
to the presence of the mentioned enzyme, which catalyzes its
degradation by randomly cleaving the 1,4 beta glycosidic bonds
between the monomeric units of the polysaccharide chain.

HAFA derivatives are resistant to the enzymatic action of
hyaluronidase, and their resistance grows with the increase of
the esterification degree.

This enzymatic degradation study was performed using the
commercial native **HA** sodium salt (molecular weight about
300 KDa) and two **HAFA** samples showing a low (**HAFA**-13,

GD = 3%) and a high esterification degree (**HAFA**-08, GD =
15%).

The experiments were carried out according to conventional
procedures. Shortly, the polysaccharide solution maintained at
37 °C (pH 7.4) and containing the enzyme in an amount equal
to 0.1 mg/mL (bovine testicular hyaluronidase, type I-S, Sigma,
1000 U/mg) was incubated at 37 °C. Two different substrate
(S)-enzyme (E) ratios (i. e. S/E = 100 and S/E = 300) were
tested. At regular time intervals, in the range 0-120 min,
samples in the amount of 0.5 mL were taken, heated at 100 °C
for 5 min, filtered to remove the enzyme, and thereafter
analyzed by means of SEC-MALS analysis in order to evaluate
the molecular weight distribution.

Already after 10 min incubation with the enzyme, the native
HA samples, at both enzyme concentrations, exhibited a rather
complete degradation, changing from an average molecular
weight of about 300 KDa to a value about 10 times lower. Also
HAFA-13 sample showed a strong degradation (i. e. 60% and
90% after 10 and 30 min of incubation) already at the lower
enzyme concentration. On the contrary, the degradation of
HAFA-08 sample was much lower [i. e. 18%, 44%, and 67% at
10, 30, and 60 min, respectively for the S/E = 300 (Figure 8)
and 29%, 61%, and 77% at the same times for the ratio S/E =
100].
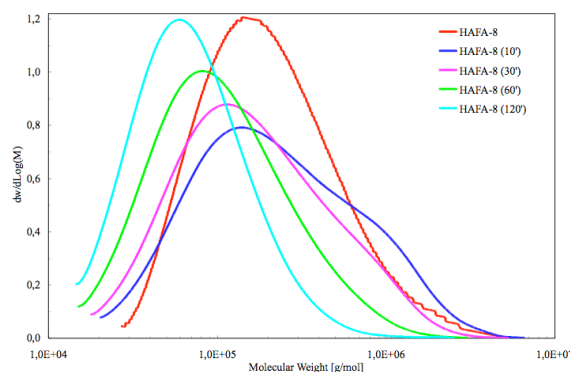
Figure 8. Comparison of differential MWD of **HAFA**-8
derivative after the enzymatic action of hyaluronidase.

Conclusions

Based on the natural feruloylation of arabinose side chains of
arabinoxylans in the cell wall of plants, a synthetic procedure
was developed in order to conjugate the natural
hydroxycinnamic acid derivative FA together with **HA**
polysaccharide macromolecule. The activation of **FA** with CDI
was extensively studied and the two reactive intermediates **2**
(monoimidazolide) and **3** (bisimidazolide) were thoroughly
characterized from the point of view of their structure and
reactivity. The easy isolation of bisimidazolide **3** as a solid
from the activation reaction mixture makes this compound an
interesting intermediate for the insertion of ferulic acid moieties
in different materials. Moreover, the reactivity characterization
by using benzyl alcohol as a model compound supports the
potential usefulness of **3** for the feruloylation of molecular or
macromolecular materials bearing hydroxyl moieties. As
expected, **3** demonstrated to be an effective reagent in the
feruloylation of **HA** producing **HAFA** graft copolymers, which

showed different grafting degrees in the range 3-17% depending on the amount of the reactants used. In particular, the stoichiometric ratio **3**/**HA** affected both GD and the conversion of **3** into ferulate in such a manner that high **3**/**HA** ratios led to relatively high GD and low conversion values, whereas a gradual decrease in GD values and an increase in the conversion percentage was obtained with the decrease of **3**/**HA** ratios. NMR studies confirmed the successful coupling between **HA** and **FA** in our reaction conditions, and the release of intact **FA** in hydrolytic conditions. The results of the macromolecular and rheological characterization of **HAFA** derivatives suggested that the grafting of **HA** with **FA** does not degrade the polysaccharide backbone and affects solubility and rheological properties. In fact, low GD values are related to high solubility and to complex viscosity values lower than those shown by native **HA** samples, whereas high GD values are linked to low solubility and higher complex viscosity values. Relatively low GD values (e. g. $\geq 8\%$) are sufficient to confer physical cross-linking properties resulting in the features of strong gel of **HAFA**-10 dispersions. Moreover, the presence of acid ferulic residues in **HAFA** derivatives produces an increased resistance to the enzymatic action of hyaluronidase, and this resistance grows with the increase of the grafting degree.

In conclusion, new materials were obtained by the covalent coupling of two natural products: a macromolecular species such as **HA** and a small molecule such as **FA**. A wide range of applications can be envisioned for these materials on the basis of the outstanding (physico-chemical, biological, and pharmacological) properties of the natural products. For instance, **HAFA** derivatives have demonstrated interesting wound healing properties both in vitro and in vivo preclinical models. Moreover, the covalent linking of **FA** to **HA** in **HAFA** graft copolymers provides additional features such as a physical cross-linking, which constitutes an added value in biological applications (e. g. as dermal fillers or in tissue engineering).

Acknowledgements

Notes and references

[a] Dipartimento di Biotecnologie, Chimica e Farmacia and European Research Centre for Drug Discovery and Development, Università degli Studi di Siena, Via A. Moro 2, 53100 Siena, Italy.

[b] Istituto per lo Studio delle Macromolecole (CNR), Via E. Bassini 15, 20133 Milano, Italy

[c] Rottapharm Madaus, Via Valosa di Sopra 7, 20900 Monza, Italy

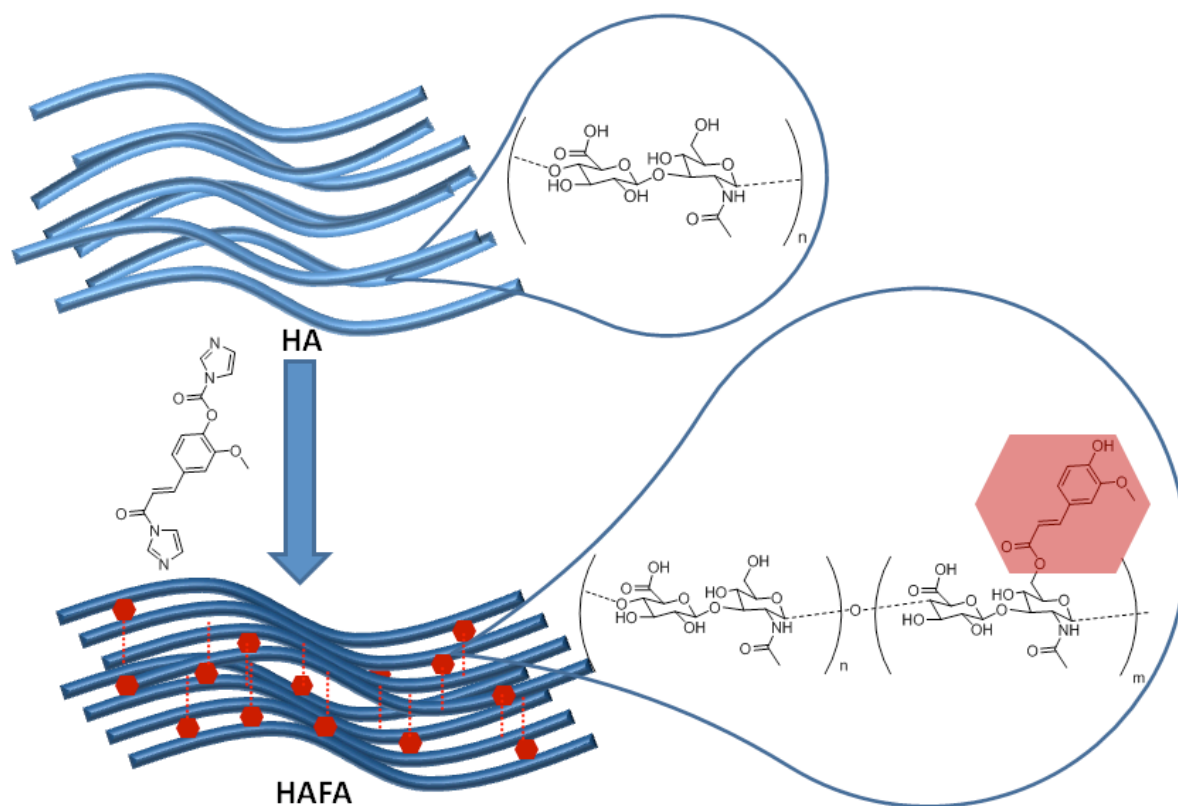*Corresponding author. Tel: +39 0577 234320. E-mail: andrea.cappelli@unisi.it.

1   A. Donati, A. Magnani, C. Bonechi, R. Barbucci and C. Rossi, *Biopolymers* 2001, **59**, 434.

2   J. A. Burdick and G. D. Prestwich, *Adv. Mater.* 2011, **23**, H41.

3   K. L. Goa and P. Benfield, *Drugs* 1994, **47**, 536.

4   T. Coviello, P. Matricardi, C. Marianecci and F. J. Alhaique, *Control. Release* 2007, **119**, 5.

5   A. Tezel and G. H. J. Fredrickson, *Cosmet. Laser Ther.* 2008, **10**, 35.

6   M. M. de O. Buanafina, *Mol. Plant* 2009, **5**, 861 and references cited therein.

7   J. H. Grabber, J. H. Ralph and R. D. Hatfield, *J. Agric. Food Chem.* 2000, **48**, 6106.

8   G. Wallace and S. Fry, *Int. Rev. Cytol.* 1994, **151**, 229.

9   S. Mathew and T. E. Abraham, *Crit. Rev. Biotechnol.* 2004, **24**, 59.

10 F. H. Lin, J. Y. Lin, R. D. Gupta, J. A. Tournas, J. A. Burch, M. Angelica Selim, N. A. Monteiro-Riviere, J. M. Grichnik, J. Zielinski, and S. R. Pinnell, *J. Invest. Dermatol.* 2005, **125**, 826.

11 S. Meyer, A. Cartelat, I. Moya, and Z. G. Cerovic, *J. Exp. Bot.* 2003, **54**, 757.

12 T. Werner and A. G. M. Barrett, *J. Org. Chem.* 2006, **71**, 4302.

13 G. Bertolini, G. Pavich, and B. Vergani, *J. Org. Chem.* 1998, **63**, 6031.

14 N. C. Nelson, A. B. Cheikh, E. Matsuda, M. M. Becker, *Biochemistry* 1996, **35**, 8429.

15 G. M. Sheldrick, SHELXS-97, Rel. 97-2, A Program for Automatic Solution of Crystal Structures, Gottingen University, 1997.

16 G. M. Sheldrick, SHELXL-97, Rel. 97-2, A Program for Crystal Structure Refinement, Gottingen University, 1997.

17 R. Mendichi, A. Giacometti Schieroni, C. Grassi, A. Re, *Polymer*, 1998, **39**, 6611.

18 R. Mendichi, A. Giacometti Schieroni, *Polymer*, 2002, **43**, 6115.

19 R. Mendichi, Giacometti A. Schieroni Use of a multi-detector size exclusion chromatography system for the characterization of complex polymers. Trans-World Research Network, S. G. Pandalai Ed., Trivandrum, India, Current Trends in Polymer Science, Vol. 6, pag. 17-32 (2001).

20 P. J. Wyatt, *Anal. Chim. Acta* 1993, **272**, 1.

21 R. Mendichi, L. Soltes, A. Giacometti Schieroni, *Biomacromolecules* 2003, **4**, 1805.

22 Recovered Mass (Recov. Mass) is the sample mass (g) eluting (i. e. recovered) from the SEC columns, expressed as % of the sample injected mass (sample concentration times injection volume). The Recovered Mass is calculated from the area of the DRI concentration detector after accurate calibration.

Journal of Materials Chemistry B Accepted Manuscript

TOC

A synthetic procedure has been developed to conjugate ferulic acid (**FA**) to an important natural polysaccharide derivative such as hyaluronic acid (**HA**).